ACCOUNTS of chemical research

pubs.acs.org/accounts Article

# Chemical Reactions at Electrified Interfaces

Shaoxin Li, Zhong Lin Wang, and Di Wei*

Cite This: *Acc. Chem. Res.* 2026, 59, 285−297 Read Online

ACCESS | Metrics & More | Article Recommendations

**CONSPECTUS:** Contact electrification (CE) is a ubiquitous interfacial phenomenon in which charge transfer occurs when two materials come into contact and subsequently separate. Remarkably, a growing body of evidence shows that CE can initiate and sustain a wide range of chemical reactions without the need for conventional thermal or photonic activation. In particular, solid−liquid CE has recently emerged as a versatile platform for sustainable chemistry, characterized by broad material compatibility, in situ radical generation, and the ability to drive diverse redox transformations. Besides, reactions occurring at gas−liquid and immiscible liquid−liquid interfaces often proceed orders of magnitude faster than in the bulk phase, underscoring the unique reactivity associated with interfacial environments. Despite these advances, the fundamental driving forces behind CE-induced chemistry remain contested, including the pathways of charge transfer and the mechanisms by which interfacial charges influence reaction coordinates. This perspective focuses on the interplay among solid−liquid CE, interfacial electron and ion transfer, and the localized triboelectric fields established during CE. By highlighting the triboelectric field as an intrinsic, tunable driving force capable of modulating interfacial reactivity, we advance the view that CE offers a distinct platform for reagent-free, sustainable chemical transformations.

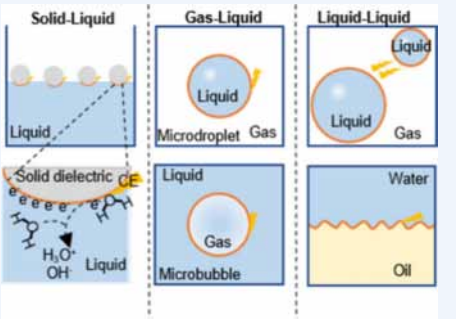




## KEY REFERENCE

- Gan, T.; Yang, Z.; Li, S.; Qian, H.; Li, Z.; Liu, J.; Peng, P.; Bai, J.; Liu, H.; Wang, Z.; Wei, D. Unveiling Janus Chemical Processes in Contact-Electro-Chemistry through Oxygen Reduction Reactions. *J. Am. Chem. Soc.* **2025**, *147*(29), 25407−25416.[1] This work establishes a comprehensive mechanistic framework for CE-chemistry, underscoring the central role of SEPs in governing its Janus redox behavior and in modulating radical reactivity in nonaqueous environments.
- Gan, T.; Li, Z.; Li, S.; Liu, H.; Amaratunga, G.; Wang, Z.; Wei, D. Sustainable Fluorinated Silicon Dielectric Design for Enhanced Contact-Electro-Chemistry. *Angew. Chem.* **2025**, *137*, e202517059.[2] This work presents fluorinated silicon (F−Si) powders as a low-cost, tunable dielectric alternative, synthesized via mild self-assembly of 1H,1H,2H,2H-perfluorodecyltriethoxysilane. F−Si achieves a 30-fold increase in methyl orange degradation over unmodified silicon and size-matched FEP.
- Liu, J.; Yang, Z.; Li, S.; Du, Y.; Zhang, Z.; Shao, J.; Willatzen, M.; Wang, Z. L.; Wei, D. Nonaqueous Contact-Electro-Chemistry via Triboelectric Charge. *J. Am. Chem. Soc.* **2024**, *146*(46), 31574−31584.[3] This work extends CE-chemistry to nonaqueous systems enables catalyst-free redox and luminescence processes. Phenol degradation in dimethyl sulfoxide (DMSO) proceeds over 40 times faster than mechanochemistry and 30 times faster than in water, where degradation remains incomplete.
- Li, S.; Zhang, Z.; Peng, P.; Li, X.; Wang, Z. L.; Wei, D. A green approach to induce and steer chemical reactions using inert solid dielectrics. *Nano Energy* **2024**, *122*, 109286.[4] This work establishes a unified paradigm of CE-chemistry, demonstrating that physical contact between solid dielectrics and liquids can induce and direct diverse reactions, including redox transformations, polymerizations, and pollutant degradations, in both aqueous and nonaqueous systems.
- Wang, Z.; Berbille, A.; Feng, Y.; Li, S.; Zhu, L.; Tang, W.; Wang, Z. L. Contact-electro-catalysis for the degradation of organic pollutants using pristine dielectric powders. *Nat. Commun.* **2022**, *13*(1), 130.[5] This work shows that electrons generated during CE between dielectric powders and water can directly catalyze reactions without traditional catalysts. Frequent CE at the fluorinated ethylene propylene (FEP)-water interface induces electron transfer, producing reactive oxygen species that degrade methyl orange.

Received: October 24, 2025
Revised: December 6, 2025
Accepted: December 23, 2025
Published: January 1, 2026





https://doi.org/10.1021/acs.accounts.5c00735
*Acc. Chem. Res.* 2026, 59, 285−297

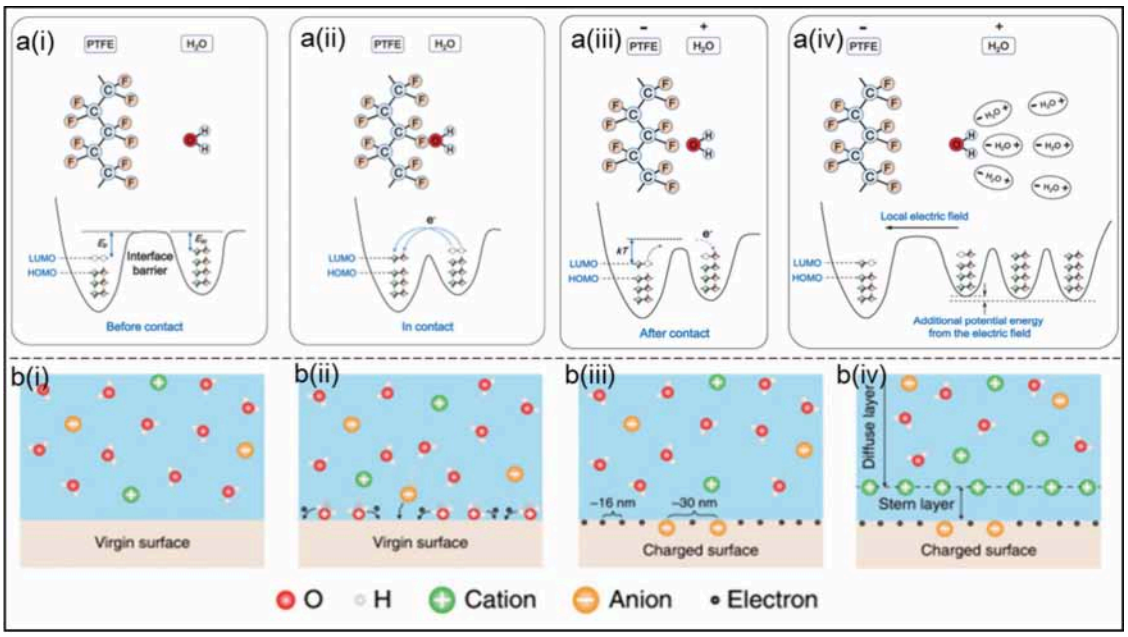


**Figure 1.** (a) Schematic diagram of electron transfer between the water molecule and PTFE molecule (copyright 2019, Wiley-VCH).[37] (b) Mechanism of liquid−solid CE and formation of EDL (copyright 2020, The Author(s)).[36]

## 1. INTRODUCTION

Contact electrification (CE) has garnered significant attention as a powerful driving force for initiating chemical reactions on triboelectrically charged solid dielectric surfaces. A comprehensive understanding of CE mechanisms at heterogeneous interfaces is pivotal for deciphering charge-transfer kinetics and enabling the rational design of interfacial reactions. When two surfaces come into contact and subsequently separate interfacial triboelectric charge accumulation often occurs. In a previous study, Liu and Bard demonstrated that CE can generate highly energetic electrons on triboelectrically charged polytetrafluoroethylene (PTFE) surfaces, which are capable of driving metal-ion reduction and electrochemiluminescent reactions.[6] Collectively, these studies underscore the decisive role of CE-induced interfacial polarity in governing chemical reactivity, establishing CE as a fundamental factor that modulates interfacial reaction pathways. For example, contact-electrocatalysis (CEC) has emerged as a novel and transformative approach that leverages charge transfer driven by CE at solid−liquid interfaces to initiate and accelerate chemical reactions.[5] This paradigm-shifting approach unlocks new possibilities for catalytic innovation by harnessing CE-induced interfacial charges as a clean, sustainable energy input for driving chemical transformations. For instance, CE-induced triboelectric charges have enabled the direct synthesis of hydrogen peroxide ($H_2O_2$) under ambient and even anaerobic conditions, without the need for costly reagents or the generation of harmful intermediates or byproducts.[7] The utility of CEC has also been extended in environmentally friendly recovery of cathode materials from spent lithium-ion batteries, achieving high leaching efficiencies of cobalt and lithium under mild, acid-free conditions.[8] In our previous studies, we extended the role of triboelectric charge into a wider range of chemical transformations, including contact-electro-redox reactions involving $[Fe(CN)_6]^{3-}/[Fe(CN)_6]^{4-}$, contact-electro-polymerization of aniline and contact-electro-fluorescence of terephthalic acid and contact-electro-luminescence of luminol.[4,9,10] Collectively, these results lead to the establishment of a broader conceptual framework, contact-electro-chemistry (CE-chemistry), which has also been successfully applied in nonaqueous systems such as dimethyl sulfoxide (DMSO).[3]

Besides, numerous studies have demonstrated that gas−liquid interfaces, such as those created by microdroplets within reaction vessels, can spontaneously promote diverse chemical transformations, including addition, elimination, and redox reactions, even in the absence of catalysts or external electric fields.[11−22] Moreover, reactions such as hydrogen−deuterium exchange and biomolecular conformational dynamics, including protein folding and unfolding, have been shown to proceed markedly faster at microdroplet interfaces than in homogeneous bulk phases.[23] Hao et al. reported that electric fields aligned along free O−H bonds at the air−water interface are about $1.6 \times 10^9$ V $m^{-1}$ stronger than those within the droplet interior.[24] Using vibrational Stark−sensitive probes and stimulated Raman excited fluorescence microscopy, Xiong et al. measured fields of $\sim 10^9$ V $m^{-1}$ at water−oil interfaces, attributed to anion adsorption−induced charge separation.[25] Similarly, Dai et al. found that biomolecular phase separation generates $\sim 5 \times 10^6$ V $m^{-1}$ fields across condensate interfaces, driving ion gradients and chemical activity.[26] These observations highlight the intrinsic chemical reactivity of interfacial environments, where local electric fields, asymmetric solvation, and nonequilibrium charge distributions can collectively lower activation barriers and alter reaction pathways.[27−29]

Notably, interfacial fields induced by CE have recently drawn attention for their comparably high electrostatic potentials arising from triboelectric charge transfer. Considering that interfacial charge transfer, including both electron and ion migration, is intimately coupled with the formation of interfacial triboelectric fields or electrical double layer (EDL). This perspective advances the concept that interfacial triboelectric fields, arising from CE, are central to initiating and steering chemical transformations. It surveys recent progress across solid−liquid, gas−liquid and liquid−liquid boundaries, with particular emphasis on how solid−liquid CE couples interfacial


https://doi.org/10.1021/acs.accounts.5c00735
Acc. Chem. Res. 2026, 59, 285−297

charge transfer and localized electric fields to govern reaction processes. Ultimately, this perspective reframes triboelectric charge into an active, tunable platform for sustainable, catalysis-free chemical transformations, offering a new paradigm for interfacial catalysis and green chemistry.

## 2. SOLID−LIQUID CE

In 1971, Kamra made a striking observation of electrostatic activity as a thunderstorm passed over the gypsum sand dunes of New Mexico.[30] At the crest of several dunes, he recorded straight, meter-high sparks shooting upward from the ground, clearly distinct from conventional thunderstorm lightning. Intriguingly, when similar strong winds occurred on days without a nearby thunderstorm, no sparks were seen. Kamra concluded that these discharges appeared only when an external electric field and sufficient humidity were present, reporting field strengths of approximately $4 \times 10^3$ V·m$^{-1}$ and relative humidity between 36% and 58%. In other words, sparks were observed in a dust storm when a thunderstorm was present, indicating strong dust-particle charging, but not under equally strong winds in fair weather.[31] This observation underscores the critical role of water vapor in enabling visible discharges within particle clouds. Although many questions remain regarding triboelectric charging mechanisms, the humidity requirement may suggest that the solid−liquid interface can sustain charge imbalance during the CE process, thereby enabling the formation of stronger interfacial triboelectric fields.

### 2.1. Charge Transfer Mechanism

As early as the 1980s, El-Kazzaz and Rose-Innes demonstrated that liquid metals in contact with insulating solids can induce surface charging on the insulator.[32] Later studies revealed that water contacting polymeric surfaces likewise generates substantial charge,[33,34] though the identity of the charge carriers in water remains complex. Despite decades of investigation, the fundamental mechanism of solid−liquid CE remains contested. This ongoing debate highlights the multifaceted character of solid−liquid CE and underscores the need for refined experimental and theoretical approaches to unravel its true origin. One of the mainstream explanations is proposed by Wang et al. solid−liquid CE is mainly governed by electron transfer arising from the overlap of electron clouds under mechanically forced contact, consistent with the "electron-cloud potential-well" model.[35] As shown in Figure 1a(i), the outer-shell electrons of oxygen(O) atom in water form a potential well, while PTFE provides a low-energy lowest unoccupied molecular orbital (LUMO) that can act as an electron acceptor. Before contact, electrons remain localized within their respective wells (Figure 1a(ii)). Upon contact, electrons can hop from the O atom of water to the PTFE LUMO, transitioning to a lower energy state and reaching equilibrium (Figure 1a(iii)). During separation, as the contact area decreases, charge density builds and the interfacial local field strengthens. If thermal energy is insufficient to overcome PTFE's energy barrier, the transferred electrons remain trapped on the PTFE surface, leaving PTFE negatively charged and water positively charged (Figure 1a(iv)). Direct experimental evidence distinguishing electron from ion transfer has been provided by Lin et al., who demonstrated that CE-generated charges removable by thermal excitation correspond to electrons, whereas ions remain surface-bound, using thermionic emission analysis combined with Kelvin probe force microscopy (KPFM).[36] The relative contribution of electrons vs ions is now described as depending systematically on (i) the liquid's ionic environment, (ii) hydrophobic/hydrophilic character of the solid, and (iii) interfacial tension and surface ionization propensity. For hydrophobic dielectrics such as PTFE, both experimental data and density functional theory (DFT) calculations indicate that electron transfer dominates.[37] This interpretation is further strengthened by the recently observed linear correlation ($R^2 \approx 0.993$) between the work function of superhydrophobic surfaces, where ion transfer is excluded, and the triboelectric charge acquired after liquid impact.[38]

### 2.2. Interfacial EDL Formation

The solid−liquid interface is not merely a passive boundary but an active platform where CE occurs through electron transfer, ion migration, and the establishment of interfacial EDL formation. Developments in the study of CE at solid−liquid interfaces have led to a paradigm shift beyond traditional electrochemical EDL models, emphasizing the critical role of electron transfer in forming the insulating solid−liquid interfacial structure. In 2018, Wang et al. proposed a hybrid EDL model with a two-step formation process that incorporates both electron transfer and ion adsorption.[36] The first stage involves molecules and ions impacts on the solid surface driven by thermal motion and liquid pressure (Figure 1b(i)), where electron cloud overlap enables electron transfer between solid atoms and water molecules (Figure 1b(ii)). Simultaneously, ionization and ion adsorption alter the local surface potential (Figure 1b(iii)). In the second stage, free ions migrate toward the charged surface under electrostatic attraction to complete the EDL (Figure 1b(iv)). The extent of EDL formation depends on the solid's electron-donating ability, consistent with known CE behavior between solids. Electrons transferred during solid−liquid collisions typically occupy surface states and are weakly bound, removable by heating, whereas those generated by ionization remain tightly bound in atomic orbitals. The EDL thus provides ionic-electronic coupling essential for controlling nanoscale process such as ion transport and interfacial field. Meanwhile, they proposed that, because water molecules are highly polarizable, the positively charged water molecule at the interface can orient and polarize neighboring water molecules through Coulombic interactions.[37] As a result, the electrostatic energy between the negatively charged PTFE surface and the interfacial water molecule is partially redistributed among the surrounding polarized molecules, effectively lowering the energetic cost required for their separation. A similar physical picture was advanced by Borwankar et al., who showed that interfacial electrostatic interactions can induce long-range, directional ordering of water molecules extending over several nanometers.[39] Moreover, the electron transfer of solid−liquid CE and its relationship to EDL formation have been elucidated through step-by-step first-principles and molecular dynamics simulations.[40] These simulations show that electron transfer generates a built-in electrostatic potential at the interface, a distinct potential drop between the solid and liquid phases. This interfacial potential acts as the driving force for ion rearrangement in the adjacent liquid, leading to EDL formation that screens the triboelectrically charged surface. These results directly support Wang's two-step model and provide detailed mechanistic insight into the coupling between CE-driven electron transfer and subsequent EDL development. Dynamic modulation of the EDL, whether by mechanical or electrostatic methods, offers new opportunities for enhancing energy


https://doi.org/10.1021/acs.accounts.5c00735
Acc. Chem. Res. 2026, 59, 285−297

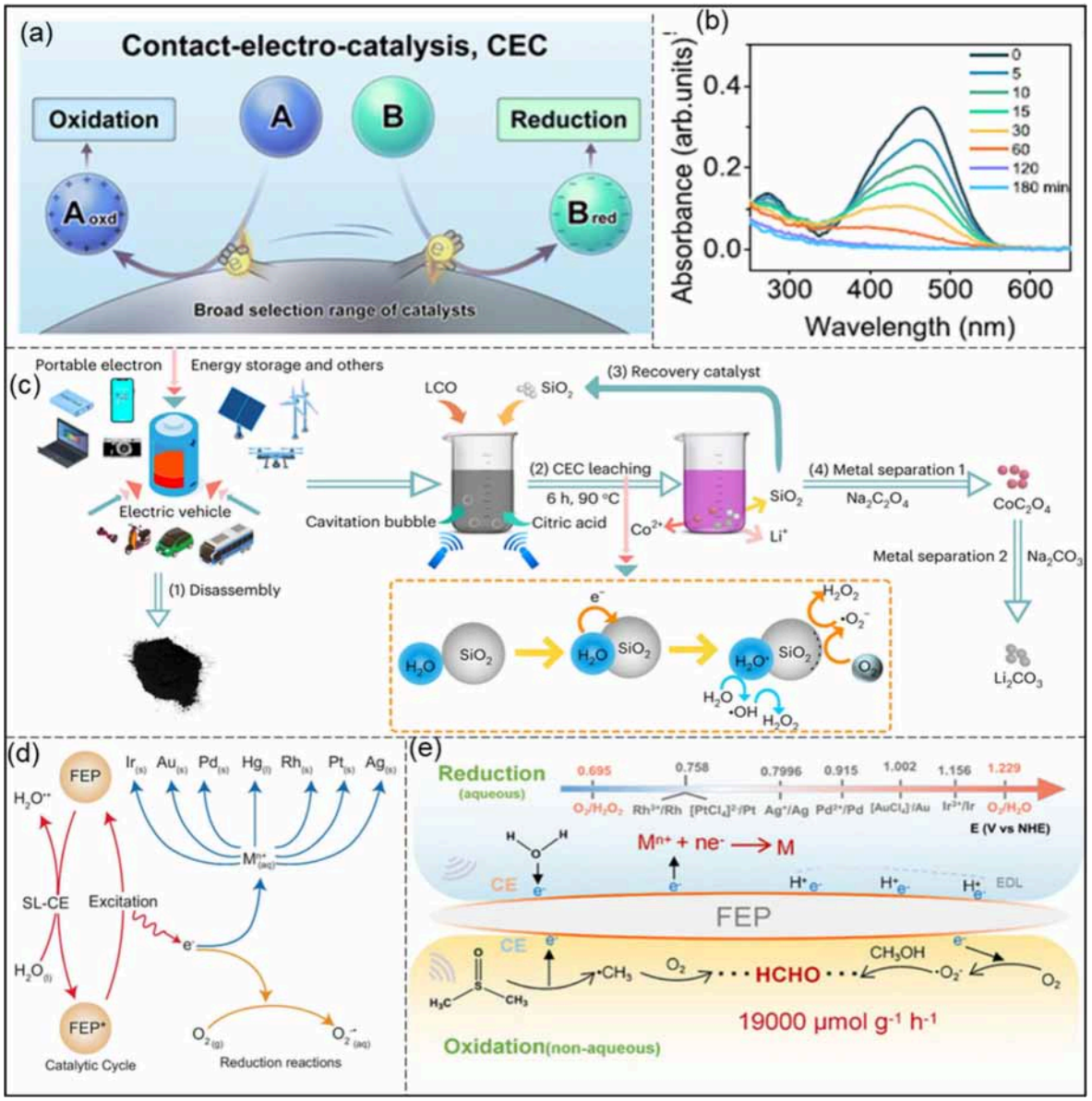


**Figure 2.** (a) The proposed mechanism of CEC (copyright 2024, American Chemical Society).[45] (b) CEC for the degradation of organic pollutants using pristine dielectric powders (copyright 2022, The Author(s)).[5] (c) A CEC cathode recycling method for spent lithium-ion batteries (copyright 2023, The Author(s), under exclusive license to Springer Nature Limited).[8] (d) Reduction of precious metal ions in aqueous solutions by CEC (copyright 2024, The Author(s)).[50] (e) Unveiling janus chemical processes in CE-chemistry through ORR. (copyright 2025, American Chemical Society).[1]

harvesting and information transfer by tuning charge carrier behavior.[41]

## 3. CHEMISTRY INITIATED BY SOLID−LIQUID CE

Once considered unpredictable and hazardous due to risks such as explosions and fire, CE is now recognized as a controllable nanoscale driving force capable of modulating diverse interfacial processes. Recent studies demonstrate that CE can be deliberately harnessed to influence wetting, adhesion, interfacial catalysis, and electrochemistry,[42−44] particularly by tuning interfacial triboelectric charge dynamics at inert solid dielectric-liquid interfaces.

### 3.1. Reactions of CE-Chemistry

Unlike conventional mechanochemistry driven purely by mechanical stress, CE-chemistry under mechanical motion with interfacial charge separation, where triboelectrically generated electric fields induce electron transfer and redox reactions. This field-driven mechanism extends mechanochemistry beyond force activation, enabling chemical transformations through dynamic interfacial polarization. Wang et al. proposed a representative CEC redox cycle (Figure 2(a)), in which reactant A transfers electrons to the catalyst surface (C) during contact, generating oxidized A and a triboelectrically charged surface (C*). C* then donates electrons to reactant B, reducing it to reductive B and regenerating C.[45] Specifically, at the FEP-water interface, electrons transfer from water to FEP, forming triboelectrically negative charged FEP, while the dissolved $O_2$ captures electrons from charged FEP to restore charge balance. Reactive oxygen species (ROS) produced during this process degrade organic pollutants such as methyl orange (MO) without added catalysts (Figure 2(b)).[5] ROS coupling further yields


https://doi.org/10.1021/acs.accounts.5c00735
Acc. Chem. Res. 2026, 59, 285−297

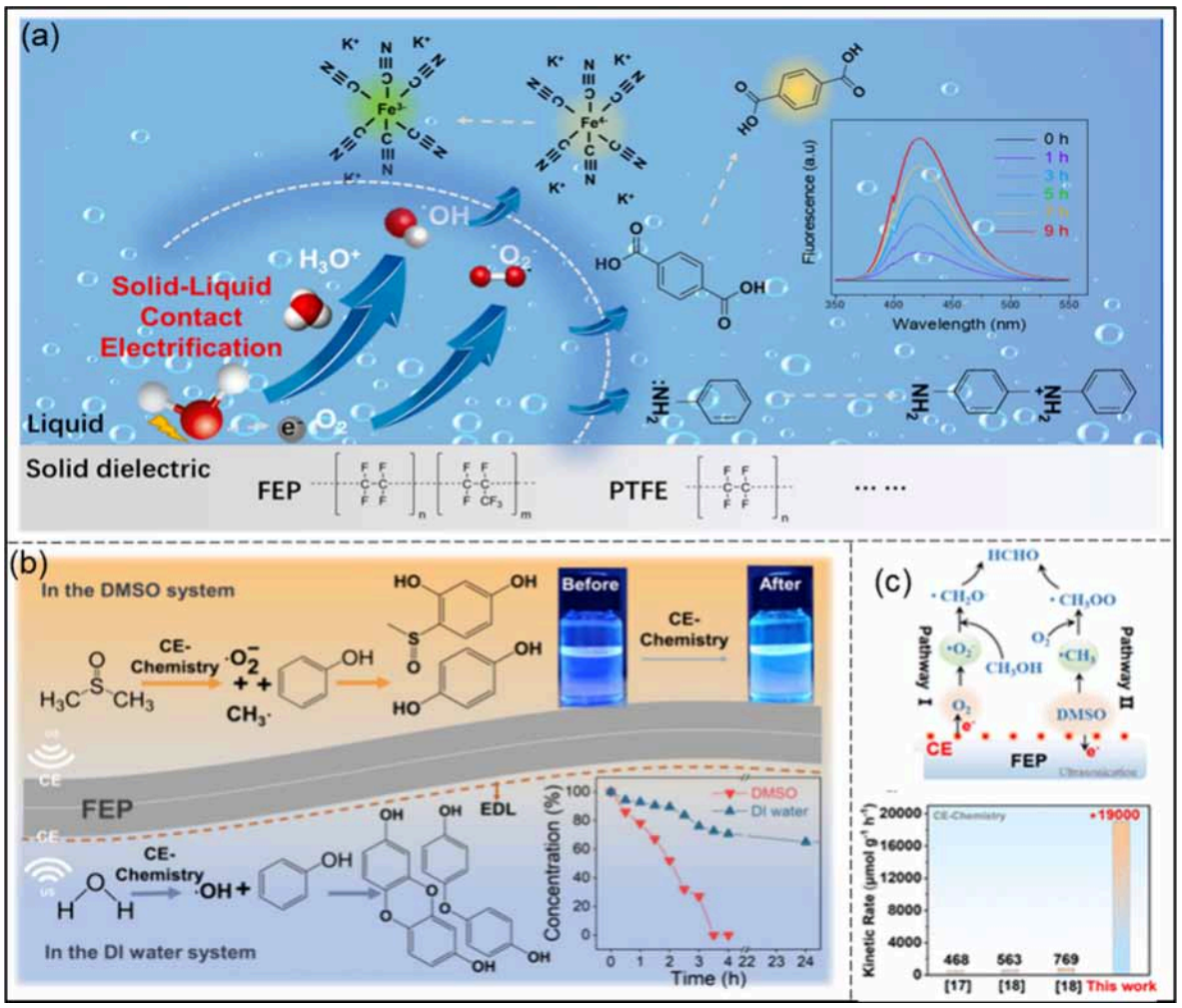


**Figure 3.** (a) A paradigm of CE-chemistry via solid−liquid CE initiates various reactions (copyright 2024 Elsevier Ltd., all rights reserved).[4] (b) Nonaqueous CE-chemistry via triboelectric charge (copyright 2024, American Chemical Society).[3] (c) $CH_3OH$ oxidation to HCHO through CE-chemistry (copyright 2025, American Chemical Society).[1]

$H_2O_2$, enabling catalyst-free synthesis under ambient conditions.[7] Recently, CEC has emerged as a powerful and sustainable route for degrading diverse emerging pollutants. Reusable PTFE particles degraded multiple antibiotics, up to 90% for tetracycline, through ·OH and $^1O_2$ pathways.[46] For persistent perfluoroalkyl substances (PFASs), contact-induced ROS generation in ultrasound/PTFE systems enabled efficient redox and defluorination of perfluorooctanoic acid (PFOA), perfluorooctanesulfonic acid (PFOS), and related species,[47] and $Bi_2WO_6$/PTFE composites achieved 90% removal of 2,4-dichlorophenol.[48] Together, these advances establish CEC as a robust, recyclable approach for eliminating antibiotics, PFASs, and other refractory contaminants. Li et al. demonstrated the use of CEC for metal extraction from spent lithium-ion batteries (Figure 2(c)).[8] Mixing $LiCoO_2$ with citric acid and silicon oxide ($SiO_2$) under ultrasonication enabled cavitation-driven contact-separation cycles that transferred electrons from water to $SiO_2$, generating ·OH, $H^+$(aq), and $\cdot O_2^-$ to promote leaching. Lithium and cobalt were recovered as $CoC_2O_4$ and $Li_2CO_3$ precursors, while $SiO_2$ was readily reused by filtration. CEC has also proven effective for uranium removal: using PTFE as the dielectric under ultrasonication, >95% of U(VI) was extracted within 5 h via CE-driven generation of electron, superoxide radicals ($\cdot O_2^-$), and $H_2O_2$, forming insoluble $(UO_2)O_2{\cdot}2H_2O$.[49] Beyond actinides, ultrasonic CEC enables reduction and recovery of $Ag^+$, $Pd^{2+}$, $[AuCl_4]^-$, $Rh^{3+}$, $Ir^{3+}$, and related metals under both aerobic and anaerobic conditions (Figure 2(d)).[50] Electron paramagnetic resonance (EPR) and ab initio studies linked CE-induced charge transfer to metal reduction, achieving gold extraction from 0.196−196 ppm solutions with capacities up to 722.5 mg $g^{-1}$ in 3 h. Collectively, these advances position CEC as a metal-free, selective, and recyclable strategy for sustainable resource recovery.

Most CE-driven studies have examined isolated oxidation (e.g., pollutant degradation) or reduction (e.g., metal-ion reduction) reactions, leaving the underlying principles of their Janus behavior, the concurrent promotion of both processes, largely unexplored. This gap obscures the mechanistic basis for reaction directionality. Wei et al. systematically investigated ultrasound-assisted CE redox processes and identified the $2e^-$ oxygen reduction reaction (ORR) as the key determinant of this duality (Figure 2(e)).[1] Reduction of metal ions (e.g., $[AuCl_4]^-$, $Pd^{2+}$, $[PtCl_4]^{2-}$, $Ag^+$, $Rh^{3+}$, and $Ir^{3+}$) was achieved when their SEPs lie above the $2e^-$ ORR ($E^\circ$ = 0.695 V vs SHE). Conversely, SEPs below the $2e^-$ ORR threshold favored oxidation (e.g., ferrocyanide). In addition to direct electron transfer from the charged solid surface, other redox-active species may also participate. For example, $Ag^+$ can be reduced both by electrons


https://doi.org/10.1021/acs.accounts.5c00735
Acc. Chem. Res. 2026, 59, 285−297

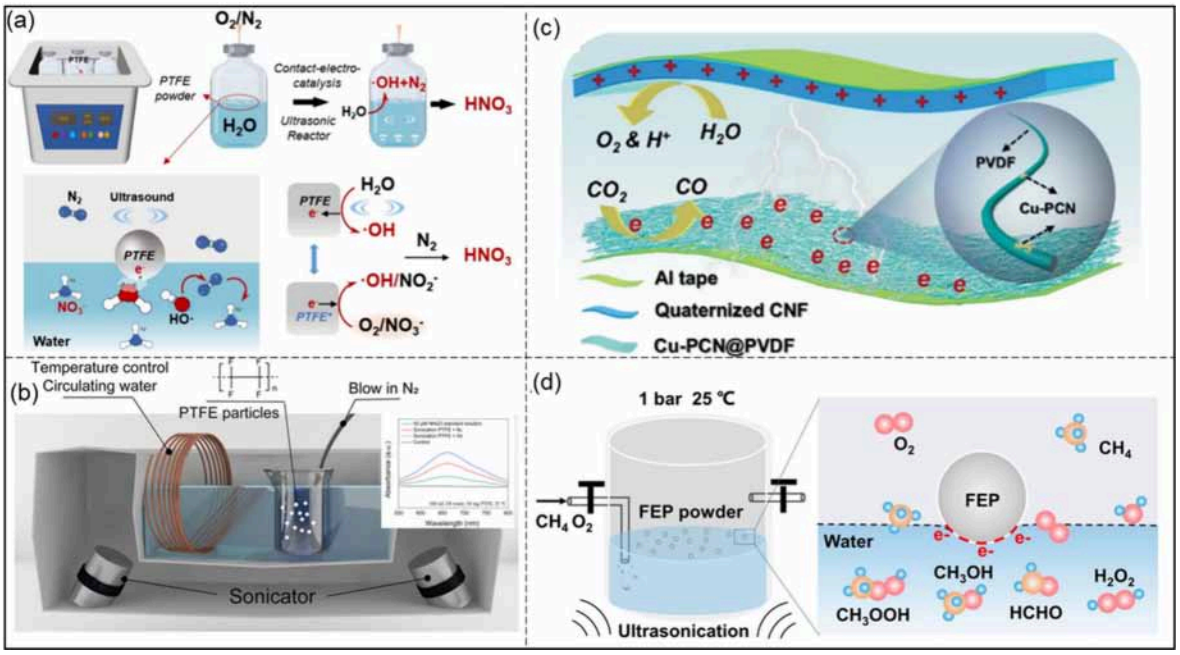


**Figure 4.** (a) Schematic of the experimental setup for $HNO_3$ production via CEC in the presence of PTFE (copyright 2025, American Chemical Society).[56] (b) Continuous ammonia synthesis from water and nitrogen via CE (copyright 2024 the Author(s)).[57] (c) $CO_2$ reduction from ambient air through CEC (copyright 2024 the Author(s)).[58] (d) CEC for direct oxidation of methane under ambient conditions (copyright 2024 Wiley-VCH GmbH).[59]

originating from the triboelectrically charged dielectric surface and by $\cdot O_2^-$ generated during CE.[51] Moreover, a synergistic interplay between $Ag^+$ reduction and MO oxidative degradation was observed, indicating coupled redox pathways operating concurrently at the interface. These findings deepen the mechanistic understanding of CE-chemistry and highlight new opportunities for exploiting synergistic catalytic processes with tunable reaction kinetics.

Solid−liquid CE has been shown to drive diverse reactions, including $[Fe(CN)_6]^{3-}/[Fe(CN)_6]^{4-}$ redox cycling, aniline polymerization, phenol degradation, and terephthalic acid fluorescence (Figure 3(a)). Building on these findings, Wei et al. introduced the unified concept of CE-chemistry, emphasizing the universality of triboelectric charge-induced transformations.[4] Moreover, they found triboelectric charges, arising even from flow electrification, can directly initiate reactions such as $[AuCl_4]^-$ reduction, luminol chemiluminescence, and $H_2O_2$ generation.[9,52] Reaction kinetics depend on dielectric geometry and flow parameters, while ROS can be tuned by dielectric type or additives (e.g., xylitol, p-benzoquinone).[10] Wei et al. later proposed that EDL buildup can inhibit CE-driven reactions.[4] In the oxidation of ferrocyanide, product yield peaked at 0.01 mM KCl and decreased at both lower and higher concentrations, revealing that excess ions suppress charge transfer. Zhan et al. confirmed that ion-rich droplets produce weaker triboelectric charging than pure water, demonstrating that EDL formation suppresses charge transfer during solid−liquid CE.[53]

Mechanistically, electron transfer from water to FEP leaves the surface negatively charged, generating $H_3O^+$ and ·OH radicals, while dissolved $O_2$ accepts electrons to form $\cdot O_2^-$, driving oxidation. As charge accumulates, hydronium adsorption forms a Stern layer that screens further electron transfer and limits $O_2$ access. These studies establish triboelectric charge as a controllable driver of interfacial reactivity, bridging CE-chemistry with electrochemistry. Analogous to conductive electrodes, an EDL forms at insulating dielectric-liquid interfaces through a two-step process: electron transfer generates surface charge, followed by ion rearrangement that screens further transfer.[42] Optimizing ion concentration or switching to nonaqueous media can overcome this effect. Using DMSO, Wei et al. demonstrated markedly enhanced CE reactivity (Figure 3(b)): phenol degradation reached 100% within 4 h versus ∼40% in water after 46 h, a >30-fold rate increase.[3] DMSO suppresses EDL formation, and enables synergistic reactions such as methanol-assisted formaldehyde generation, ∼25 times higher than in water (Figure 4(c)).[1] These findings highlight solvent selection as a key lever to modulate EDL effects, radical speciation, and CE-chemistry efficiency.

In addition, multiple independent studies now demonstrate that CE at solid−liquid can directly drive redox reactions. Hu et al. showed that dielectric-water contact can continuously generate $H_2O_2$ and electrical power via CE-driven interfacial electron transfer.[54] More recently, Wang et al. demonstrated $O_2$-independent $H_2O_2$ production from water−polymer CE, confirming that water−polymer CE can function as an autonomous chemical driving force rather than a secondary consequence of flow or cavitation.[55] Collectively, these studies reinforce the broader principle that CE at solid−liquid interfaces is capable of acting as a genuine driving force for redox transformations.

### 3.2. Interfacial Reactions of CE-Chemistry

In CE-chemistry, the surrounding gas environment plays a pivotal role by dictating how triboelectric charges on solid dielectrics are consumed. $O_2$, for instance, can capture interfacial electrons to form $\cdot O_2^-$ radicals that promote pollutant degradation while competing with metal-ion reduction. Gases may also act directly as reactants: Huang and co-workers recently achieved ambient nitrogen fixation to $HNO_3$ via ultrasonically driven contact between PTFE and water, without


https://doi.org/10.1021/acs.accounts.5c00735
Acc. Chem. Res. 2026, 59, 285−297

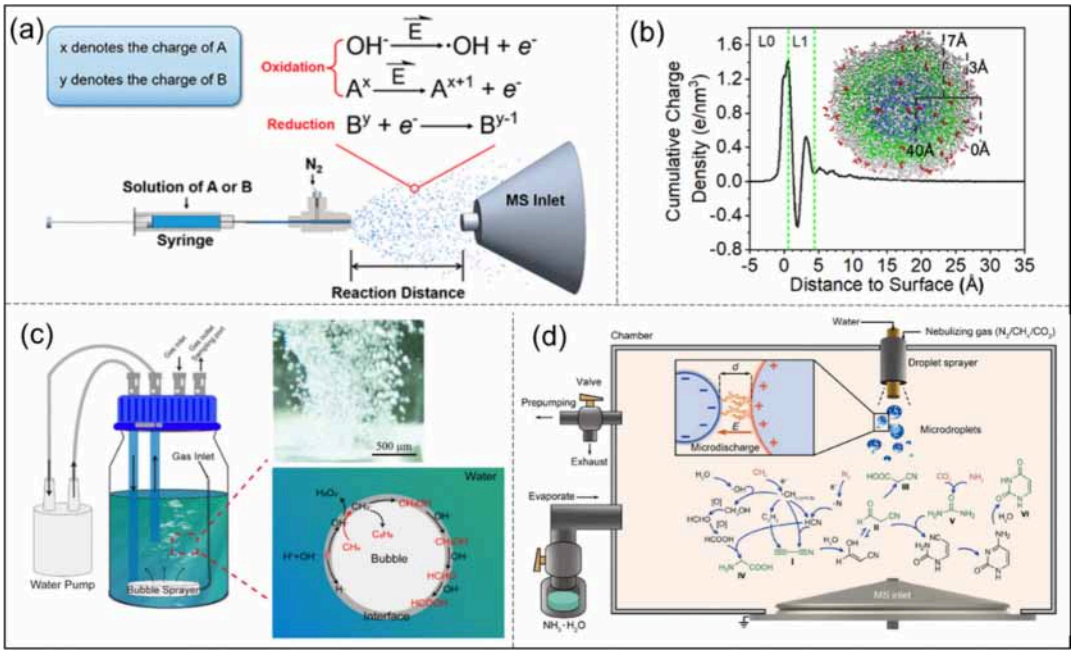


**Figure 5.** (a) Setup of a typical mass spectrometry experiment for microdroplet chemistry and the electron-mediated redox mechanisms that occur at the air−water interface of the droplets (copyright 2023 The Authors).[18] (b) Cumulative charge density using the ReaxFF/C-GeM model (copyright 2022, The Author(s)).[24] (c) Methane C($sp^3$)-H bond activation by water microbubbles (copyright 2024, CC BY-NC 3.0).[70] (d) Spraying of water microdroplets forms luminescence and causes chemical reactions in surrounding gas (copyright 2025, The American Association for the Advancement of Science).[75]

external bias or light (Figure 4a).[56] The process attains production rates of 6.9 ± 1.3 $\mu$M $h^{-1}$ under pure nitrogen and 40.7 ± 1.8 $\mu$M $h^{-1}$ under air, driven by ·OH radicals generated through water oxidation and oxygen reduction. Reaction efficiency depends sensitively on PTFE dosage, particle size, and interfacial area. Isotopic labeling and high-resolution mass spectrometry (HRMS) analyses confirmed ·OH-mediated nitrogen activation, establishing CE-chemistry as a distinct, energy-free route to nitrogen fixation. Zare and co-workers reported an ambient-condition route for ammonia synthesis by bubbling nitrogen through an aqueous suspension of PTFE particles (~5 $\mu$m, ~50 mg in 200 mL, stabilized with 0.05 vol % Tween-20) at 25 °C (Figure 4(b)).[57] Ammonia formation was attributed to nitrogen activation and reduction driven by CE-induced electron transfer at the solid−liquid interface. Under ultrasonic agitation and near-neutral pH (6.5−7.0), the system achieved an $NH_3$ production rate of ≈420 $\mu$mol $L^{-1}$ $h^{-1}$ $g^{-1}$ PTFE. Incorporating PTFE into titanium dioxide ($TiO_2$) via hydrothermal synthesis produced a $TiO_2$@PTFE hybrid catalyst that couples mechanical and optical energy inputs.[Shi, 2024 #496] This composite enabled sustainable nitrogen fixation under ambient conditions without sacrificial agents, reaching 133.6 $\mu$mol $g^{-1}$ $h^{-1}$ activity. Together, these advances highlight the potential of synergistic CE and photodriven strategies for green ammonia production.

CEC has also emerged as a promising strategy to address key challenges in carbon dioxide ($CO_2$) reduction. Wang and co-workers developed a triboelectric nanogenerator (TENG) system achieving a Faradaic efficiency of 96.2% for carbon monoxide (CO) production with a yield of 33 $\mu$mol $g^{-1}$ $h^{-1}$ (Figure 4(c)).[58] In this design, a positively charged quaternized cellulose nanofiber (CNF) layer captures $CO_2$ via hydrogen bonding and generates protons through water oxidation, while a negatively charged polyvinylidene fluoride (PVDF) layer embedded with single-atom Cu on polymeric carbon nitride (Cu-PCN) provides active sites for $CO_2$ reduction. Triboelectric charges produced during contact-separation cycles drive electron transfer from Cu-PCN to adsorbed $CO_2$, coupling capture, proton generation, and redox conversion into a single, bias-free process. Extending this concept, Fan et al. demonstrated methane activation via ultrasonic electrification of FEP in water (Figure 4(d)),[59] directly converting methane ($CH_4$) and $O_2$ into methanol ($CH_3OH$) and HCHO with yields of 151.2 and 467.5 $\mu$mol $g^{-1}$, respectively. EPR detected ·OH and $\cdot O_2^-$ radicals, while isotope mass spectrometry confirmed $CH_3OH$ formation and its subsequent oxidation to methanal (HCHO).[59]

## 4. CHEMISTRY AT LIQUID SURFACES

### 4.1. Microdroplet Chemistry

In recent years, unusual behaviors of water microdroplets have attracted increasing attention. Rapid and spontaneous formation of gold nanoparticles (AuNPs) and nanowires has been reported in aerosol microdroplets, even without reducing agents or templates.[60] At the air−water interface, water oxidation generates $H_2O_2$, as evidenced by strong peroxyfluor-1 fluorescence in atomized microdroplets (1−20 $\mu$m) but not in bulk solution, with smaller droplets yielding higher signals.[61] A broad range of mechanisms has been proposed to account for the unusual chemistry observed at microdroplet interfaces,[22] including enhanced interfacial concentration,[62] partial solvation,[63] gas-phase partitioning and reactions,[64] accelerated evaporation,[65] etc. Time-resolved imaging revealed that $H_2O_2$ generation in microdroplets is governed by droplet curvature and interfacial electrostatics.[66] Real-time mass spectrometry further showed one-step, catalyst-free oxidation of alcohols to $ROO^-$ intermediates on microdroplet surfaces under ambient conditions.[67] The accumulation of hydroperoxide ions at the air−water boundary indicates that intrinsic surface potentials


https://doi.org/10.1021/acs.accounts.5c00735
Acc. Chem. Res. 2026, 59, 285−297

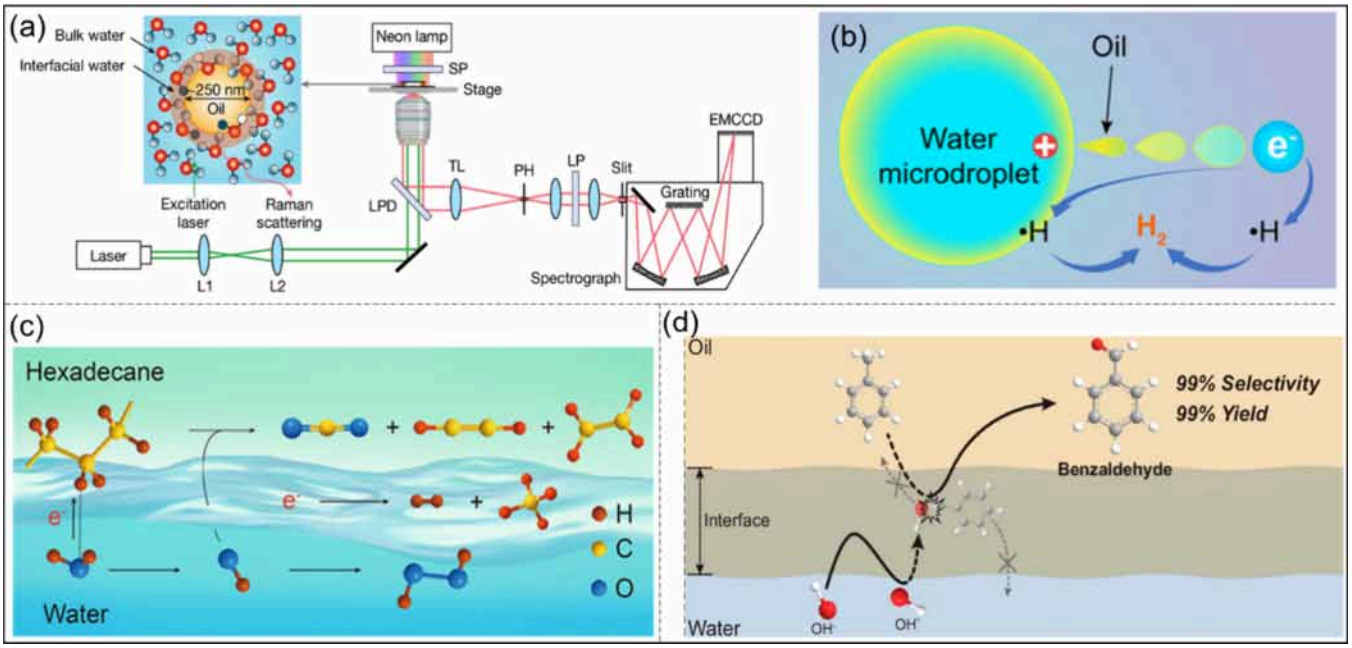


**Figure 6.** (a) Schematic of custom-built confocal micro-Raman system (copyright 2025, The Author(s), under exclusive license to Springer Nature Limited).[89] (b) Sprayed oil−water microdroplets as a hydrogen source (copyright 2024, American Chemical Society).[92] (c) Hydrocarbon degradation by contact with anoxic water microdroplets (copyright 2023, American Chemical Society).[93] (d) Catalyst-free selective oxidation of C($sp^3$)-H bonds in toluene on water (copyright 2024, The Author(s)).[94]

promote asymmetric charge separation and water oxidation, driving interfacial alcohol oxidation.[68] A broad range of redox reactions can thus be initiated by interfacial electric fields through electron abstraction from $OH^-$, producing ·OH radicals and free electrons (Figure 5(a)).[18] Although average interfacial fields at the air−water interface reach $\sim 1.6 \times 10^9$ V $m^{-1}$, Hao et al. showed that reaction acceleration cannot be explained by field magnitude alone (Figure 5(b)).[24] Instead, fluctuations in the electrostatic potential, arising from the dynamic restructuring of interfacial solvation shells, lower the activation barrier for ·OH formation, as confirmed by first-principles molecular dynamics simulations.[69]

Inspired by the pronounced reactivity of water microdroplets, a microbubble system was designed to probe gas−liquid interfacial oxidation and methane C−H activation (Figure 5(c)).[70] The enlarged interfacial area of microbubbles promotes the generation of ·OH and H· radicals, initiating methane activation and yielding $CH_3$· intermediates that couple to form ethane and formic acid. Although bubble formation in electrochemical systems is often regarded as a parasitic process reducing active surface area, the gas−water interface itself carries intrinsic electrostatic potential.[71] Zeta potential measurements further showed that bubbles in ultrapure water possess negative charge due to $OH^-$ enrichment, establishing an interfacial potential gradient that extends into the aqueous phase.[72] Moreover, Zhou et al. demonstrated that charged microdroplet sprays can activate and dissociate dioxygen, generating ozone anions ($O_3^-$) without catalysts.[73] Intense interdroplet electric fields and transient "microlightning" events between oppositely charged droplets drive O−O bond cleavage and ROS formation. High-speed imaging under uniform fields provides direct evidence of the Lenard effect, revealing smaller negatively charged droplets and larger positively charged ones.[74] Localized electric fields approaching $\sim 10^9$ V $m^{-1}$ arise between such droplets, promoting charge transfer and even gas ionization, as confirmed by open-air mass spectrometry detecting $N_2^+$, $O_2^+$, $NO^+$, and $NO_2^+$. Meng et al. further observed spontaneous luminescence from sprayed water droplets without applied bias,[75] indicating microlightning sufficient to excite or ionize nearby molecules. Remarkably, spraying room-temperature water microdroplets into nitrogen, methane, carbon dioxide, and ammonia mixtures produced C−N-containing organic compounds (Figure 5(d)), reminiscent of Urey-Miller-type prebiotic synthesis.

Studies has also suggested that CE contributes to the intrinsic electrification of microdroplet surfaces.[68] Supporting this view, recent work on gas−liquid TENG architectures demonstrates that two-phase flows can generate substantial electrical outputs through contact and inductive electrification, with voltages ranging from hundreds to several thousand volts depending on hydrodynamic conditions and device geometry.[76] Remarkably, controlled gas−liquid interfaces in Venturi-type and atomization systems can sustain continuous charge separation, with as little as 1 mL of liquid capable of illuminating more than 1,500 LEDs.[77−79] Furthermore, bubble-driven two-phase flows have been shown to generate output voltages of tens of volts using underwater bubble-based generators.[80−82] Chen et al. reported that sprayed microdroplets undergo $H_2O_2$ formation through · OH radicals recombination initiated by water−solid CE.[83] Xia et al. further revealed that interactions between silicate surfaces and water vapor produce ROS over extended time scales, again attributing the chemistry to CE-mediated charge transfer at gas/solid−water boundaries.[84] These findings indicate that gas−liquid CE can produce significant surface charge densities and interfacial electric fields capable of driving redox processes.[85] Dynamic contact-separation cycles inherent to droplet breakup, coalescence, and jet−air interactions can rapidly accumulate charge at curved gas−liquid interfaces. Several experimental studies report local interfacial fields of $10^8$−$10^9$ V $m^{-1}$ in highly curved microdroplets, sufficient to oxidize $OH^-$ to ·OH and to


https://doi.org/10.1021/acs.accounts.5c00735
Acc. Chem. Res. 2026, 59, 285−297

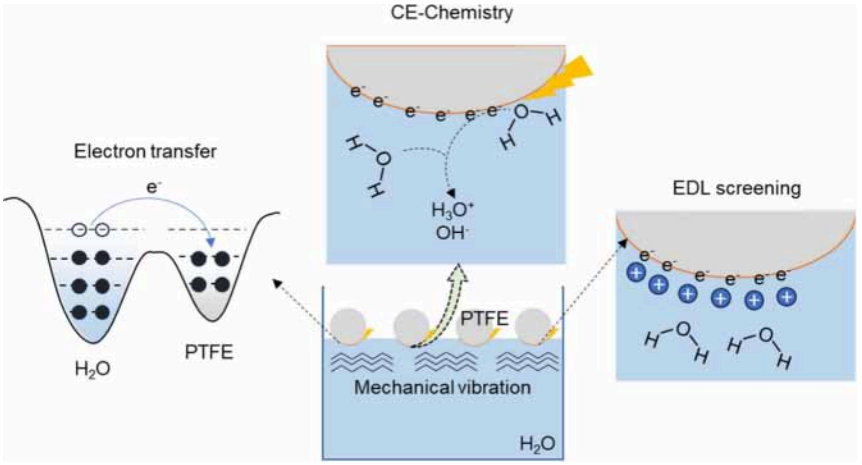


**Figure 7.** Schematic illustration of triboelectric charge transfer at CE-chemistry.

generate $H_2O_2$ spontaneously.[61,86] While not definitive, these observations suggest that CE-induced electron transfer may constitute one mechanistic contributor to reaction acceleration and selectivity in charged microdroplets.

### 4.2. Chemistry at Immiscible Liquid Interfaces

At water-hydrophobic interfaces, water orientation, ionic enrichment, hydrogen-bond disruption, and strong interfacial electric fields have been widely observed.[87,88] Shi et al. used interface-selective Raman spectroscopy with multivariate analysis and a monomer-field model to probe hexadecane-in-water emulsions (Figure 6(a)).[89] They found reduced tetrahedral order, weakened hydrogen bonding, and abundant free hydroxyl groups with a ∼95 $cm^{-1}$ red shift relative to planar oil−water interfaces. From the known zeta potential of oil droplets,[90] the interfacial field was estimated at $\sim(5-9) \times 10^9$ V $m^{-1}$, arising from charge separation in the oil phase. Xiong et al. quantified ∼ $10^9$ V $m^{-1}$ electric fields at water−oil interfaces using vibrational Stark spectroscopy, attributing them to charge separation from preferential anion adsorption during ultrasonication.[25,91] Charge and EPR measurements revealed that CE at oil−water microdroplet interfaces extracts electrons from water, enhancing charge separation and neutralization.[92] The process yields ∼13-fold more charge carriers than pure water sprays and a ∼16-fold increase in hydrogen production for selective $CO_2$-to-CO conversion, underscoring the potential of emulsified systems to drive hydrogenation reactions (Figure 6(b)). Chen et al. further showed that water−oil charge transfer produces $H_2$, $CO_2$, and short-chain hydrocarbons in emulsified water-hexadecane mixtures (Figure 6(c)).[93] At similar interfaces, Lee et al. achieved catalyst-free oxidation of toluene via · OH radicals, where interfacial OH groups extending into the oil phase favored H-abstraction over addition, yielding benzaldehyde with >99% selectivity under mild conditions (Figure 6(d)).[94] Together, these studies highlight how triboelectric fields at immiscible liquid boundaries govern interfacial redox and catalytic reactivity. Dai et al. further reported electric fields of ∼5 × $10^6$ V/m at the liquid−liquid interface between biomolecular condensates and surrounding bulk solution, strong enough to drive in situ redox reactions in vitro and in living systems, underscoring interfacial electric fields as active electrochemical environments.[26] Moreover, their recent studies have revealed that biomolecular condensates, membraneless assemblies with strong interfacial electric fields, can catalyze hydrolysis reactions by modulating local water activity and electric potentials at phase boundaries, suggesting that similar field-driven chemistry may operate at immiscible liquid interfaces in biological systems.[95]

## 5. PERSPECTIVE

Systematic analysis shows that chemical activity in CE-chemistry arises from interfacial electron transfer and the consequent formation of a nanoscale, localized electric field, here termed the triboelectric field. Its magnitude is governed by the electronegativity or chemical-potential difference between the contacting phases. In the PTFE-water system, for example, PTFE's higher electronegativity drives electron accumulation on the polymer surface, generating a negative interfacial potential and a spatially confined triboelectric field across the PTFE-water boundary. The initial step in solid−liquid CE is dominantly governed by electron transfer driven by electron-cloud overlap under mechanically enforced contact, consistent with the "electron-cloud potential-well" model proposed by Wang and co-workers.[35] Following electron transfer, the triboelectrically charged dielectric surface electrostatically redistributes nearby ions, leading to counterion accumulation and the formation of a nascent EDL. Although analogous to the EDL at electrochemical interfaces, this structure is fundamentally distinct because the dielectric is nonconductive and no external bias is applied. At elevated ionic strengths, this EDL rapidly screens the surface charge, producing pronounced EDL suppression of subsequent CE-driven electron transfer.[37]

Importantly, before the EDL is fully established, repeated contact-separation cycles permit continued charge accumulation on the dielectric surface as the continue CE of PTFE-water, progressively increasing its negative potential while rendering the adjacent liquid phase increasingly positive. Upon nanoscale separation, this charge asymmetry gives rise to a highly confined transient triboelectric field, experimentally evidenced by macroscopic air-gap breakdown events observed during PTFE-water CE at atmospheric pressure.[96] Because air breakdown occurs at $\sim 3 \times 10^6$ V $m^{-1}$, the interfacial field within the nanometer-scale CE contact zone must be substantially higher, sufficient to lower reaction barriers and activate otherwise inaccessible interfacial redox pathways. Furthermore, it was recently shown by Jin et al. that the electrostatic field generated during CEC is sufficiently strong to drive C−F bond cleavage in perfluoroalkyl substances. Because the SEP for C−F dissociation is approximately $E^\circ$ = −2.755 V vs SHE,[97] this reaction can proceed only if the local


https://doi.org/10.1021/acs.accounts.5c00735
Acc. Chem. Res. 2026, 59, 285−297

interfacial potential difference reaches several volts. Consistent with this requirement, the authors measured PTFE surface potentials of −2 to −10 V after high-pressure water impingement (0.1−0.5 bar). If this potential drop is confined within a subnanometre reaction zone, the corresponding instantaneous interfacial field is on the order of $10^9$−$10^{10}$ V $m^{-1}$, which is comparable to the interfacial electric fields ∼$10^9$ V $m^{-1}$ of conductive electrode−electrolyte interfaces in electrochemistry.[98−100] Recent 3D atomic force microscopy (3D-AFM) and theoretical studies showed that altering surface charge via CE markedly reorganizes hydration-layer structure, demonstrating that CE-generated triboelectric fields modulate interfacial water at the atomic scale.[101] Besides, their in situ experiments showed that the oscillation of the hydration layer caused by CE is comparable to that observed in electrochemical systems. It is important to note that these two systems differ fundamentally in origin: whereas electrochemical interfaces require an externally applied potential to a conductive electrode, solid dielectric-liquid interfaces can spontaneously develop strong interfacial triboelectric fields under mechanical stimulation. These triboelectric fields are fully capable of initiating redox processes that are mechanistically analogous to electrochemical Faradaic reactions, yet they proceed without any applied bias, arising solely from CE-driven electron transfer and the subsequent radical-mediated chemical reactions.

Therefore, we have now clarified that this transient triboelectric field precedes and is later moderated by EDL formation (Figure 7). During this transient window, the triboelectric field can polarize interfacial solvent molecules, reorganize hydrogen-bond networks, and initiate redox processes through triboelectric electrons and radical intermediates. CE-generated electrons stored on PTFE surface, for example, can directly reduce metal ions in the absence of external bias.[50] The resulting redox selectivity follows the SEP of the reactant, establishing a predictable threshold that separates oxidative from reductive regimes.[1] The solvent environment further modulates radical speciation: ·OH radicals dominate in water, whereas methyl (·$CH_3$) radicals form in DMSO.[3] Collectively, the selective generation of radicals, solvent-dependent product distribution, and SEP-correlated redox behavior demonstrate that the triboelectric field functions as an intrinsic driving force, one that polarizes interfacial solvent molecules, redistributes ions, and lowers activation barriers to enable redox and radical transformations.

In conclusion, triboelectrically charged solid−liquid interfaces exhibit catalytic activity driven by dynamic CE. Highly electronegative dielectrics, such as fluorinated polymers, efficiently extract electrons from liquids, producing ROS that mediate subsequent transformations. In addition to direct charge transfer, CE induces persistent surface charges that create intense interfacial triboelectric fields. Solid−liquid CE can generate voltages of hundreds to thousands of volts, corresponding to nanoscale fields strong enough to polarize molecules and enable metal-free, field-driven chemical activation at quasi-electrode surfaces. Despite these advances, probing and controlling triboelectric fields at solid−liquid interfaces CE remain challenging. Progress will require refined experimental techniques and theoretical models to accurately measure interfacial triboelectric field strength and spatial distribution, track their dynamic evolution during CE, and enable their deliberate modulation to control chemical reactivity. Strategies that mitigate EDL shielding, such as the use of aprotic, nonaqueous solvents, may be can enhance charge accessibility and improve reaction efficiency. Looking forward, rational design of solid−liquid CE interfaces through the control of dielectric properties, surface chemistry, and morphology presents a promising paradigm for metal-free, sustainable catalysis. Realizing this potential will require multidisciplinary efforts integrating operando spectroscopy, theoretical modeling, and nanoscale electrochemical mapping to elucidate the spatiotemporal evolution of interfacial charge, triboelectric fields distribution, and reaction dynamics. Collectively, these advances position interfacial triboelectric fields as autonomous, programmable triggers for chemical transformations, opening new frontiers in catalysis, synthetic chemistry, energy conversion, and environmental remediation.

## AUTHOR INFORMATION


### Corresponding Author

**Di Wei** − *Beijing Institute of Nanoenergy and Nanosystems, Chinese Academy of Sciences, Beijing 101400, P. R. China; Centre for Photonic Devices and Sensors, University of Cambridge, Cambridge CB3 0FA, UKNEH;* orcid.org/0000-0003-2670-6362; Email: weidi@binn.cas.cn

### Authors

**Shaoxin Li** − *Beijing Institute of Nanoenergy and Nanosystems, Chinese Academy of Sciences, Beijing 101400, P. R. China; School of Nanoscience and Engineering, University of Chinese Academy of Sciences, Beijing 100049, P. R. China; Department of Chemistry, Stanford University, Stanford, California 94305, United States*

**Zhong Lin Wang** − *Beijing Institute of Nanoenergy and Nanosystems, Chinese Academy of Sciences, Beijing 101400, P. R. China*

Complete contact information is available at: https://pubs.acs.org/10.1021/acs.accounts.5c00735


### Notes

The authors declare no competing financial interest.

### Biographies

**Shaoxin Li** achieved the Ph.D degree from the University of Chinese Academy of Sciences. She is a postdoctoral at the University of Chinese Academy of Sciences, and visiting postdoctoral at Stanford University. Her research interest is self-powered sensors, energy harvesting, and solid−liquid contact electrification.

**Zhong Lin Wang** received his PhD degree in Physics from Arizona State University. He is the Director of the Beijing Institute of Nanoenergy and Nanosystems and Regents' Professor and Hightower Chair at the Georgia Institute of Technology. He pioneered the nanogenerators field for distributed energy, self-powered sensors, and large-scale blue energy.

**Di Wei** received his PhD degree in electroanalytical Chemistry from Åbo Akademi University. He serves as the Principal Investigator at BINN and heads the Iontronics Laboratory. As Fellow of the Royal Society of Chemistry (FRSC) and Senior Member of Wolfson College at Cambridge University. His research focus on controlling ionic currents, which underpin numerous scientific and technological advancements, serving as carriers of energy and information as well as probes for reaction kinetics.


https://doi.org/10.1021/acs.accounts.5c00735
Acc. Chem. Res. 2026, 59, 285−297

## ■ ACKNOWLEDGMENTS

This work was supported by the National Natural Science Foundation (grant number 22479016).

## ■ REFERENCES

(1) Gan, T.; Yang, Z.; Li, S.; Qian, H.; Li, Z.; Liu, J.; Peng, P.; Bai, J.; Liu, H.; Wang, Z.; Wei, D. Unveiling Janus Chemical Processes in Contact-Electro-Chemistry through Oxygen Reduction Reactions. *J. Am. Chem. Soc.* **2025**, *147* (29), 25407−25416.
(2) Gan, T.; Li, Z.; Li, S.; Liu, H.; Amaratunga, G.; Wang, Z.; Wei, D. Sustainable Fluorinated Silicon Dielectric Design for Enhanced Contact-Electro-Chemistry. *Angew. Chem.* **2025**, *137*, e202517059.
(3) Liu, J.; Yang, Z.; Li, S.; Du, Y.; Zhang, Z.; Shao, J.; Willatzen, M.; Wang, Z. L.; Wei, D. Nonaqueous Contact-Electro-Chemistry via Triboelectric Charge. *J. Am. Chem. Soc.* **2024**, *146* (46), 31574−31584.
(4) Li, S.; Zhang, Z.; Peng, P.; Li, X.; Wang, Z. L.; Wei, D. A green approach to induce and steer chemical reactions using inert solid dielectrics. *Nano Energy* **2024**, *122*, 109286.
(5) Wang, Z.; Berbille, A.; Feng, Y.; Li, S.; Zhu, L.; Tang, W.; Wang, Z. L. Contact-electro-catalysis for the degradation of organic pollutants using pristine dielectric powders. *Nat. Commun.* **2022**, *13* (1), 130.
(6) Liu, C.; Bard, A. J. Electrostatic electrochemistry at insulators. *Nat. Mater.* **2008**, *7* (6), 505−509.
(7) Zhao, J.; Zhang, X.; Xu, J.; Tang, W.; Lin Wang, Z.; Ru Fan, F. Contact-electro-catalysis for Direct Synthesis of H2O2 under Ambient Conditions. *Angew. Chem., Int. Ed.* **2023**, *62* (21), No. e202300604.
(8) Li, H.; Berbille, A.; Zhao, X.; Wang, Z.; Tang, W.; Wang, Z. L. A contact-electro-catalytic cathode recycling method for spent lithium-ion batteries. *Nature Energy* **2023**, *8* (10), 1137−1144.
(9) Xu, C.; Li, S.; Zhang, Y.; Wang, Z.; Wang, Z. L.; Wei, D. Contact-electro-chemistry induced by flow electrification in dielectric tubes. *Nano Energy* **2025**, *134*, No. 110526.
(10) Xu, C.; Li, S.; Yang, Z.; Willatzen, M.; Lin Wang, Z.; Wei, D. Contact-electro-luminescence triggered by triboelectric charge. *Chemical Engineering Journal* **2024**, *501*, No. 157754.
(11) Xing, D.; Yuan, X.; Liang, C.; Jin, T.; Zhang, S.; Zhang, X. Spontaneous oxidation of I− in water microdroplets and its atmospheric implications. *Chem. Commun.* **2022**, *58* (89), 12447−12450.
(12) Zhang, D.; Yuan, X.; Gong, C.; Zhang, X. High Electric Field on Water Microdroplets Catalyzes Spontaneous and Ultrafast Oxidative C−H/N−H Cross-Coupling. *J. Am. Chem. Soc.* **2022**, *144* (35), 16184−16190.
(13) Gong, C.; Li, D.; Li, X.; Zhang, D.; Xing, D.; Zhao, L.; Yuan, X.; Zhang, X. Spontaneous Reduction-Induced Degradation of Viologen Compounds in Water Microdroplets and Its Inhibition by Host−Guest Complexation. *J. Am. Chem. Soc.* **2022**, *144* (8), 3510−3516.
(14) Qiu, L.; Cooks, R. G. Simultaneous and Spontaneous Oxidation and Reduction in Microdroplets by the Water Radical Cation/Anion Pair. *Angew. Chem., Int. Ed.* **2022**, *61* (41), No. e202210765.
(15) Song, X.; Meng, Y.; Zare, R. N. Spraying Water Microdroplets Containing 1,2,3-Triazole Converts Carbon Dioxide into Formic Acid. *J. Am. Chem. Soc.* **2022**, *144* (37), 16744−16748.
(16) Chen, H.; Wang, R.; Xu, J.; Yuan, X.; Zhang, D.; Zhu, Z.; Marshall, M.; Bowen, K.; Zhang, X. Spontaneous Reduction by One Electron on Water Microdroplets Facilitates Direct Carboxylation with CO2. *J. Am. Chem. Soc.* **2023**, *145* (4), 2647−2652.
(17) Yuan, X.; Zhang, D.; Liang, C.; Zhang, X. Spontaneous Reduction of Transition Metal Ions by One Electron in Water Microdroplets and the Atmospheric Implications. *J. Am. Chem. Soc.* **2023**, *145* (5), 2800−2805.
(18) Jin, S.; Chen, H.; Yuan, X.; Xing, D.; Wang, R.; Zhao, L.; Zhang, D.; Gong, C.; Zhu, C.; Gao, X.; Chen, Y.; Zhang, X. The Spontaneous Electron-Mediated Redox Processes on Sprayed Water Microdroplets. *JACS Au* **2023**, *3* (6), 1563−1571.
(19) He, Q.; Zhang, N.; Qiao, Y.; Li, C.; Zhang, J. Vapor generation of mercury and methylmercury in aqueous microdroplets produced by pneumatic nebulization. *Journal of Analytical Atomic Spectrometry* **2022**, *37* (9), 1894−1901.
(20) Mohajer, M. A.; Basuri, P.; Evdokimov, A.; David, G.; Zindel, D.; Miliordos, E.; Signorell, R. Spontaneous formation of urea from carbon dioxide and ammonia in aqueous droplets. *Science* **2025**, *388* (6754), 1426−1430.
(21) Layman, B. R.; Carrel, D. M.; Dick, J. E. Multiphase Electrochemiluminescence of Microdroplets and Radical Salts. *Acc. Chem. Res.* **2025**, *58* (12), 1856−1866.
(22) LaCour, R. A.; Heindel, J. P.; Zhao, R.; Head-Gordon, T. The Role of Interfaces and Charge for Chemical Reactivity in Microdroplets. *J. Am. Chem. Soc.* **2025**, *147* (8), 6299−6317.
(23) Wei, Z.; Li, Y.; Cooks, R. G.; Yan, X. Accelerated Reaction Kinetics in Microdroplets: Overview and Recent Developments. *Annu. Rev. Phys. Chem.* **2020**, *71*, 31−51.
(24) Hao, H.; Leven, I.; Head-Gordon, T. Can electric fields drive chemistry for an aqueous microdroplet? *Nat. Commun.* **2022**, *13* (1), 280.
(25) Xiong, H.; Lee, J. K.; Zare, R. N.; Min, W. Strong Electric Field Observed at the Interface of Aqueous Microdroplets. *J. Phys. Chem. Lett.* **2020**, *11* (17), 7423−7428.
(26) Dai, Y.; Chamberlayne, C. F.; Messina, M. S.; Chang, C. J.; Zare, R. N.; You, L.; Chilkoti, A. Interface of biomolecular condensates modulates redox reactions. *Chem.* **2023**, *9* (6), 1594−1609.
(27) Girod, M.; Moyano, E.; Campbell, D. I.; Cooks, R. G. Accelerated bimolecular reactions in microdroplets studied by desorption electrospray ionization mass spectrometry. *Chemical Science* **2011**, *2* (3), 501−510.
(28) Yan, X. Emerging microdroplet chemistry for synthesis and analysis. *Int. J. Mass Spectrom.* **2021**, *468*, No. 116639.
(29) Lee, J. K.; Kim, S.; Nam, H. G.; Zare, R. N. Microdroplet fusion mass spectrometry for fast reaction kinetics. *Proc. Natl. Acad. Sci. U. S. A.* **2015**, *112* (13), 3898−3903.
(30) Kamra, A. K. Physical Sciences: Visual Observation of Electric Sparks on Gypsum Dunes. *Nature* **1972**, *240* (5377), 143−144.
(31) Lacks, D. J. Frictile attraction. *Nat. Phys.* **2010**, *6* (5), 324−325.
(32) El-Kazzaz, A.; Rose-Innes, A. C. Contact charging of insulators by liquid metals. *J. Electrostat.* **1985**, *16*, 157−163.
(33) Matsui, M.; Murasaki, N.; Fujibayashi, K.; Bao, P. Y.; Kishimoto, Y. Electrification of pure water flowing down a trough set up with a resin sheet. *J. Electrost.* **1993**, *31* (1), 1−10.
(34) Yatsuzuka, K.; Mizuno, Y.; Asano, K. Electrification phenomena of pure water droplets dripping and sliding on a polymer surface. *J. Electrost.* **1994**, *32* (2), 157−171.
(35) Xu, C.; Zi, Y.; Wang, A. C.; Zou, H.; Dai, Y.; He, X.; Wang, P.; Wang, Y. C.; Feng, P.; Li, D. On the electron-transfer mechanism in the contact-electrification effect. *Advanced materials* **2018**, *30* (15), No. 1706790.
(36) Lin, S.; Xu, L.; Chi Wang, A.; Wang, Z. L. Quantifying electron-transfer in liquid-solid contact electrification and the formation of electric double-layer. *Nat. Commun.* **2020**, *11* (1), 399.
(37) Nie, J.; Ren, Z.; Xu, L.; Lin, S.; Zhan, F.; Chen, X.; Wang, Z. L. Probing Contact-Electrification-Induced Electron and Ion Transfers at a Liquid−Solid Interface. *Adv. Mater.* **2020**, *32* (2), No. 1905696.
(38) Jin, Y.; Yang, S.; Sun, M.; Gao, S.; Cheng, Y.; Wu, C.; Xu, Z.; Guo, Y.; Xu, W.; Gao, X. How liquids charge the superhydrophobic surfaces. *Nat. Commun.* **2024**, *15* (1), 4762.
(39) Marinova, K. G.; Alargova, R. G.; Denkov, N. D.; Velev, O. D.; Petsev, D. N.; Ivanov, I. B.; Borwankar, R. P. Charging of Oil−Water Interfaces Due to Spontaneous Adsorption of Hydroxyl Ions. *Langmuir* **1996**, *12* (8), 2045−2051.
(40) Wu, J.; Cao, J.; Bi, H.; Zhang, J.; Cao, Q. Liquid-solid contact electrification and its effect on the formation of electric double layer: An atomic-level investigation. *Nano Energy* **2023**, *111*, No. 108442.
(41) Li, X.; Wang, Z. L.; Wei, D. Scavenging Energy and Information through Dynamically Regulating the Electrical Double Layer. *Adv. Funct. Mater.* **2024**, *34* (42), No. 2405520.
(42) Lin, S.; Chen, X.; Wang, Z. L. Contact Electrification at the Liquid−Solid Interface. *Chem. Rev.* **2022**, *122* (5), 5209−5232.


https://doi.org/10.1021/acs.accounts.5c00735
*Acc. Chem. Res.* 2026, 59, 285−297

(43) Galembeck, F.; Santos, L. P.; Burgo, T. A. L.; Galembeck, A. The emerging chemistry of self-electrified water interfaces. *Chem. Soc. Rev.* **2024**, *53* (5), 2578−2602.
(44) Wang, X.; Lin, F.; Wang, X.; Fang, S.; Tan, J.; Chu, W.; Rong, R.; Yin, J.; Zhang, Z.; Liu, Y.; Guo, W. Hydrovoltaic technology: from mechanism to applications. *Chem. Soc. Rev.* **2022**, *51* (12), 4902−4927.
(45) Wang, Z.; Dong, X.; Tang, W.; Wang, Z. L. Contact-electrocatalysis (CEC). *Chem. Soc. Rev.* **2024**, *53* (9), 4349−4373.
(46) Cao, D.-Q.; Fang, R.-K.; Song, Y.-X.; Ma, M.-G.; Li, H.; Hao, X.-D.; Wu, R.; Chen, X. Contact-electro-catalysis for degradation of trace antibiotics in wastewater. *Chemical Engineering Journal* **2024**, *487*, No. 150531.
(47) Wang, Y.; Zhang, J.; Zhang, W.; Yao, J.; Liu, J.; He, H.; Gu, C.; Gao, G.; Jin, X. Electrostatic Field in Contact-Electro-Catalysis Driven C−F Bond Cleavage of Perfluoroalkyl Substances. *Angew. Chem., Int. Ed.* **2024**, *63* (19), No. e202402440.
(48) Wu, M.; Zhang, Y.; Yi, Y.; Zhou, B.; Sun, P.; Dong, X. Regulation of friction pair to promote conversion of mechanical energy to chemical energy on $Bi_2WO_6$ and realization of enhanced tribocatalytic activity to degrade different pollutants. *Journal of Hazardous Materials* **2023**, *459*, No. 132147.
(49) Dai, Z.; Chen, L.; Liang, B.; Li, L.; Ding, D. Efficient extraction of uranium(VI) in aqueous solution by contact-electro-catalysis. *Chemical Engineering Journal* **2024**, *502*, No. 157893.
(50) Su, Y.; Berbille, A.; Li, X.-F.; Zhang, J.; PourhosseiniAsl, M.; Li, H.; Liu, Z.; Li, S.; Liu, J.; Zhu, L.; Wang, Z. L. Reduction of precious metal ions in aqueous solutions by contact-electro-catalysis. *Nat. Commun.* **2024**, *15* (1), 4196.
(51) Shah, M.; Li, S.; Yang, Z.; Liu, J.; Peng, P.; Qian, H.; Wang, Z. L.; Wei, D. Synergistic effects in triboelectric charge-driven redox reactions. *Nano Energy* **2025**, *144*, No. 111380.
(52) Lee, K.; Bose, S.; Song, X.; Choi, S. Q.; Zare, R. N. Continuous Flow Contact Electrocatalysis for Hydrogen Peroxide Production. *J. Phys. Chem. C* **2025**, *129* (13), 6254−6261.
(53) Zhan, F.; Wang, A. C.; Xu, L.; Lin, S.; Shao, J.; Chen, X.; Wang, Z. L. Electron Transfer as a Liquid Droplet Contacting a Polymer Surface. *ACS Nano* **2020**, *14* (12), 17565−17573.
(54) Hu, Y.; Yang, W.; Ma, Y.; Qiu, Y.; Wei, W.; Wu, B.; Li, K.; Li, Y.; Zhang, Q.; Xiao, R.; Hou, C.; Wang, H. Solid-liquid interface charge transfer for generation of $H_2O_2$ and energy. *Nat. Commun.* **2025**, *16* (1), 1692.
(55) Wang, Y.; Wei, P.; Shen, Z.; Wang, C.; Ding, J.; Zhang, W.; Jin, X.; Vecitis, C. D.; Gao, G. O2-Independent $H_2O_2$ Production via Water−Polymer Contact Electrification. *Environ. Sci. Technol.* **2024**, *58* (1), 925−934.
(56) Huang, S.; Liu, Y.; Ren, L.; Huang, L.; Tang, J.; Yu, Z.; Chen, M.; Zhou, S. Direct Conversion of N2 to Nitric Acid via Contact Electrocatalysis. *ACS Sustainable Chem. Eng.* **2025**, *13* (27), 10486−10494.
(57) Li, J.; Xia, Y.; Song, X.; Chen, B.; Zare, R. N. Continuous ammonia synthesis from water and nitrogen via contact electrification. *Proc. Natl. Acad. Sci. U. S. A.* **2024**, *121* (4), No. e2318408121.
(58) Wang, N.; Jiang, W.; Yang, J.; Feng, H.; Zheng, Y.; Wang, S.; Li, B.; Heng, J. Z. X.; Ong, W. C.; Tan, H. R. Contact-electro-catalytic CO2 reduction from ambient air. *Nat. Commun.* **2024**, *15* (1), 5913.
(59) Li, W.; Sun, J.; Wang, M.; Xu, J.; Wang, Y.; Yang, L.; Yan, R.; He, H.; Wang, S.; Deng, W.-Q.; Tian, Z.-Q.; Fan, F. R. Contact-Electro-Catalysis for Direct Oxidation of Methane under Ambient Conditions. *Angew. Chem., Int. Ed.* **2024**, *63* (20), No. e202403114.
(60) Lee, J. K.; Samanta, D.; Nam, H. G.; Zare, R. N. Spontaneous formation of gold nanostructures in aqueous microdroplets. *Nat. Commun.* **2018**, *9* (1), 1562.
(61) Lee, J. K.; Walker, K. L.; Han, H. S.; Kang, J.; Prinz, F. B.; Waymouth, R. M.; Nam, H. G.; Zare, R. N. Spontaneous generation of hydrogen peroxide from aqueous microdroplets. *Proc. Natl. Acad. Sci. U. S. A.* **2019**, *116* (39), 19294−19298.
(62) Xiong, H.; Lee, J. K.; Zare, R. N.; Min, W. Strong Concentration Enhancement of Molecules at the Interface of Aqueous Microdroplets. *J. Phys. Chem. B* **2020**, *124* (44), 9938−9944.
(63) Qiu, L.; Wei, Z.; Nie, H.; Cooks, R. G. Reaction Acceleration Promoted by Partial Solvation at the Gas/Solution Interface. *ChemPlusChem.* **2021**, *86* (10), 1362−1365.
(64) Jacobs, M. I.; Davis, R. D.; Rapf, R. J.; Wilson, K. R. Studying Chemistry in Micro-compartments by Separating Droplet Generation from Ionization. *J. Am. Soc. Mass Spectrom.* **2019**, *30* (2), 339−343.
(65) Lai, Y.-H.; Sathyamoorthi, S.; Bain, R. M.; Zare, R. N. Microdroplets Accelerate Ring Opening of Epoxides. *J. Am. Soc. Mass Spectrom.* **2018**, *29* (5), 1036−1043.
(66) Lee, K.; Mehrgardi, M. A.; Zare, R. N. Interfacial Curvature, not Simply Size, Controls Spontaneous Hydrogen Peroxide Formation in Water Microdroplets. *J. Am. Chem. Soc.* **2025**, *147* (36), 33240−33247.
(67) Mofidfar, M.; Mehrgardi, M. A.; Zare, R. N. Water Microdroplets Surrounded by Alcohol Vapor Cause Spontaneous Oxidation of Alcohols to Organic Peroxides. *J. Am. Chem. Soc.* **2024**, *146* (27), 18498−18503.
(68) Mehrgardi, M. A.; Mofidfar, M.; Zare, R. N. Sprayed Water Microdroplets Are Able to Generate Hydrogen Peroxide Spontaneously. *J. Am. Chem. Soc.* **2022**, *144* (17), 7606−7609.
(69) Martins-Costa, M. T. C.; Ruiz-López, M. F. Electrostatics and Chemical Reactivity at the Air−Water Interface. *J. Am. Chem. Soc.* **2023**, *145* (2), 1400−1406.
(70) Li, J.; Xu, J.; Song, Q.; Zhang, X.; Xia, Y.; Zare, R. N. Methane C(sp3)−H bond activation by water microbubbles. *Chemical Science* **2024**, *15* (41), 17026−17031.
(71) Chaplin, M. F. Theory vs experiment: what is the surface charge of water. *WATER* **2009**, *1*, 1−28.
(72) Takahashi, M. ζ Potential of Microbubbles in Aqueous Solutions: Electrical Properties of the Gas−Water Interface. *J. Phys. Chem. B* **2005**, *109* (46), 21858−21864.
(73) Zhou, J.; Wang, Q.; Cheng, G.; Shen, W.; Zare, R. N.; Sun, X. Charged Water Microdroplets Enable Dissociation of Surrounding Dioxygen. *J. Am. Chem. Soc.* **2025**, *147* (13), 10916−10924.
(74) Xia, Y.; Xu, J.; Li, J.; Chen, B.; Dai, Y.; Zare, R. N. Visualization of the Charging of Water Droplets Sprayed into Air. *J. Phys. Chem. A* **2024**, *128* (28), 5684−5690.
(75) Meng, Y.; Xia, Y.; Xu, J.; Zare, R. N. Spraying of water microdroplets forms luminescence and causes chemical reactions in surrounding gas. *Science Advances* **2025**, *11* (11), No. eadt8979.
(76) Wang, F.; Yang, P.; Tao, X.; Shi, Y.; Li, S.; Liu, Z.; Chen, X.; Wang, Z. L. Study of Contact Electrification at Liquid-Gas Interface. *ACS Nano* **2021**, *15* (11), 18206−18213.
(77) Dong, Y.; Feng, M.; Cheng, J.; Chang, S.; Wang, D.; Lu, W. Ring-shaped single-electrode triboelectric nanogenerator (RSE-TENG) for energy harvesting and liquid flow rate monitoring of gas-liquid two-phase flow. *Nano Energy* **2024**, *119*, No. 109083.
(78) Wu, Q.; Wang, W.; Zhang, L.; Wu, X.; Zhang, X.; Wang, D. High-output pulsed water flow and gas-liquid two-phase flow triboelectric nanogenerator based on induction electrification. *Nano Energy* **2024**, *126*, No. 109642.
(79) Li, C.; Qin, Y.; Zhang, H.; Wang, Y.; Liao, J.; Guo, H. Spray power generation based on triboelectric effect. *Nano Energy* **2024**, *120*, No. 109138.
(80) Yan, X.; Xu, W.; Deng, Y.; Zhang, C.; Zheng, H.; Yang, S.; Song, Y.; Li, P.; Xu, X.; Hu, Y.; Zhang, L.; Yang, Z.; Wang, S.; Wang, Z. Bubble energy generator. *Science Advances* **2022**, *8* (25), No. eabo7698.
(81) Du, Y.; Guan, Z.; Chen, D.; Ye, J.; Li, P.; Wen, Y. Broadband rotary hybrid generator for wide-flow-rate fluid energy harvesting and bubble power generation. *Energy Conversion and Management* **2021**, *250*, No. 114833.
(82) Yan, X.; Song, Y.; Zheng, H.; Cui, H.; Wang, Z.; Xu, W. A bubble energy generator featuring lubricant-impregnated surface with high durability and efficiency. *Nano Energy* **2024**, *121*, No. 109238.
(83) Chen, B.; Xia, Y.; He, R.; Sang, H.; Zhang, W.; Li, J.; Chen, L.; Wang, P.; Guo, S.; Yin, Y.; Hu, L.; Song, M.; Liang, Y.; Wang, Y.; Jiang, G.; Zare, R. N. Water−solid contact electrification causes hydrogen peroxide production from hydroxyl radical recombination in sprayed microdroplets. *Proc. Natl. Acad. Sci. U. S. A.* **2022**, *119* (32), No. e2209056119.


https://doi.org/10.1021/acs.accounts.5c00735
*Acc. Chem. Res.* 2026, 59, 285−297

(84) Xia, Y.; Li, J.; Zhang, Y.; Yin, Y.; Chen, B.; Liang, Y.; Jiang, G.; Zare, R. N. Contact between water vapor and silicate surface causes abiotic formation of reactive oxygen species in an anoxic atmosphere. *Proc. Natl. Acad. Sci. U. S. A.* **2023**, *120* (30), No. e2302014120.
(85) Dong, Y.; Xu, S.; Zhang, C.; Zhang, L.; Wang, D.; Xie, Y.; Luo, N.; Feng, Y.; Wang, N.; Feng, M.; Zhang, X.; Zhou, F.; Wang, Z. L. Gas-liquid two-phase flow-based triboelectric nanogenerator with ultrahigh output power. *Science Advances* **2022**, *8* (48), No. eadd0464.
(86) Lin, S.; Cao, L. N. Y.; Tang, Z.; Wang, Z. L. Size-dependent charge transfer between water microdroplets. *Proc. Natl. Acad. Sci. U. S. A.* **2023**, *120* (31), No. e2307977120.
(87) Strazdaite, S.; Versluis, J.; Backus, E. H. G.; Bakker, H. J. Enhanced ordering of water at hydrophobic surfaces. *J. Chem. Phys.* **2014**, *140* (5), 054711.
(88) Yang, S.; Chen, M.; Su, Y.; Xu, J.; Wu, X.; Tian, C. Stabilization of hydroxide ions at the interface of a hydrophobic monolayer on water via reduced proton transfer. *Phys. Rev. Lett.* **2020**, *125* (15), No. 156803.
(89) Shi, L.; LaCour, R. A.; Qian, N.; Heindel, J. P.; Lang, X.; Zhao, R.; Head-Gordon, T.; Min, W. Water structure and electric fields at the interface of oil droplets. *Nature* **2025**, *640* (8057), 87−93.
(90) Roger, K.; Cabane, B. Why are hydrophobic/water interfaces negatively charged? *Angew. Chem., Int. Ed.* **2012**, *51* (23), 5625.
(91) Lee, J. K.; Han, H. S.; Chaikasetsin, S.; Marron, D. P.; Waymouth, R. M.; Prinz, F. B.; Zare, R. N. Condensing water vapor to droplets generates hydrogen peroxide. *Proc. Natl. Acad. Sci. U. S. A.* **2020**, *117* (49), 30934−30941.
(92) Chen, X.; Xia, Y.; Wu, Y.; Xu, Y.; Jia, X.; Zare, R. N.; Wang, F. Sprayed Oil−Water Microdroplets as a Hydrogen Source. *J. Am. Chem. Soc.* **2024**, *146* (15), 10868−10874.
(93) Chen, X.; Xia, Y.; Zhang, Z.; Hua, L.; Jia, X.; Wang, F.; Zare, R. N. Hydrocarbon Degradation by Contact with Anoxic Water Microdroplets. *J. Am. Chem. Soc.* **2023**, *145* (39), 21538−21545.
(94) Lee, K.; Cho, Y.; Kim, J. C.; Choi, C.; Kim, J.; Lee, J. K.; Li, S.; Kwak, S. K.; Choi, S. Q. Catalyst-free selective oxidation of C(sp3)-H bonds in toluene on water. *Nat. Commun.* **2024**, *15* (1), 6127.
(95) Chen, M. W.; Guo, X.; Farag, M.; Qian, N.; Song, X.; Ni, A.; Liu, V.; Yu, X.; Ma, Y.; Yang, L.; Yu, W.; King, M. R.; Lee, J.; Zare, R. N.; Min, W.; Pappu, R. V.; Dai, Y. Condenzymes: Biomolecular condensates with inherent catalytic activities. *bioRxiv* 2025, DOI: 10.1101/2024.07.06.602359.
(96) Ye, C.; Liu, D.; Gao, Y.; Liu, F.; Xu, H.; Jiang, T.; Wang, Z. L. Electrostatic breakdown at liquid-solid-gas triple-phase interfaces owing to contact electrification. *Matter* **2025**, *8* (4), 102007.
(97) Röckl, J. L.; Robertson, E. L.; Lundberg, H. Electrosynthetic C−F bond cleavage. *Organic & Biomolecular Chemistry* **2022**, *20* (34), 6707−6720.
(98) Clark, M. L.; Ge, A.; Videla, P. E.; Rudshteyn, B.; Miller, C. J.; Song, J.; Batista, V. S.; Lian, T.; Kubiak, C. P. CO2 Reduction Catalysts on Gold Electrode Surfaces Influenced by Large Electric Fields. *J. Am. Chem. Soc.* **2018**, *140* (50), 17643−17655.
(99) Zeradjanin, A. R.; Vimalanandan, A.; Polymeros, G.; Topalov, A. A.; Mayrhofer, K. J. J.; Rohwerder, M. Balanced work function as a driver for facile hydrogen evolution reaction − comprehension and experimental assessment of interfacial catalytic descriptor. *Phys. Chem. Chem. Phys.* **2017**, *19* (26), 17019−17027.
(100) Schmickler, W. Electronic Effects in the Electric Double Layer. *Chem. Rev.* **1996**, *96* (8), 3177−3200.
(101) Tang, Z.; Lin, S.; Wang, Z. L. Unveiling Contact-Electrification Effect on Interfacial Water Oscillation. *Adv. Mater.* **2024**, *36* (44), No. 2407507.




https://doi.org/10.1021/acs.accounts.5c00735
Acc. Chem. Res. 2026, 59, 285−297